



The adsorption of CO on transition metal clusters: A case study of cluster surface chemistry

André Fielicke^{a,*}, Philipp Gruene^a, Gerard Meijer^a, David M. Rayner^b

^aFritz-Haber-Institut der Max-Planck-Gesellschaft, Faradayweg 4-6, D-14195 Berlin, Germany

^bSteacie Institute for Molecular Sciences, National Research Council, 100 Sussex Drive, Ottawa, Ontario, Canada K1A 0R6

ARTICLE INFO

Article history:

Available online 20 January 2009

Keywords:

Vibrational spectroscopies
Infrared absorption spectroscopy
Chemisorption, Surface chemical reaction
Vibrations of adsorbed molecules
Carbon monoxide
Metal clusters

ABSTRACT

We present a discussion of recent experimental studies on the interaction of single CO molecules with transition metal clusters in the gas-phase, typically in the size range of 3 to more than 20 atoms, emphasizing specifically the insights gained from vibrational spectroscopy. Trends across the transition metals (TM) for molecular vs. dissociative chemisorption as well as for adsorption geometries are discussed and compared with the behaviour of CO adsorbed on extended surfaces. The dependence of the frequency of the internal CO stretch vibration on the size and charge of the cluster enables one to gauge *quantitatively* the effects of charge transfer between deposited nanoparticles and the substrate as well as of electron transfer due to the binding of co-adsorbed species.

© 2009 Elsevier B.V. All rights reserved.

1. Introduction

Shortly after the synthesis of polynuclear metal compounds in inorganic chemistry in the 1960 and 70s [1] these cluster compounds have been proposed as molecular model systems for the chemisorption on extended metal surfaces [2]. Later, the development of laser ablation techniques to generate metal clusters in the gas-phase brought a new perspective to this approach [3]. The analogy between a metal surface and small clusters containing typically only between 2 and 10 atoms has been conceptually fruitful to gain insights into interactions between a metal center and organic and inorganic reactants.

The carbon monoxide molecule, CO, is one of the most widely studied ligands, in cluster chemistry as well as in surface science. Its binding mechanism to transition metals (TM) is well understood [4,5] and can be described in terms of σ -donation of electron density from CO to the metal and π -backdonation from the metal to CO, according to the Blyholder model [6]. Moreover, the chemistry of CO is of great interest as CO oxidation and hydrogenation reactions are among the most important TM catalyzed reactions. It is known that the catalytic activity can be heavily dependent on the particle size of the catalyst used [7]. Finally, the C–O stretching frequency, $\nu(\text{CO})$, is highly sensitive to the nature of the binding site and its local electron density. Measuring $\nu(\text{CO})$ by means of infrared (IR) spectroscopy has long been used in order to study binding sites of CO on TM surfaces and on technical cata-

lysts [8,9]. Recently, such techniques have been used to study the interaction of CO with metal particles of definite size, which have been either deposited size-selectively [10,11] or characterized after deposition using microscopic techniques [12,13].

A large variety of TM carbonyl cluster compounds can be prepared and handled in macroscopic quantities. These cluster compounds are often considered as models for the CO adsorption on extended metal surfaces, although all or a major fraction of metal atoms interact directly with the ligand molecules and the properties of the metal core can be significantly altered compared to that of a naked cluster. These ligand stabilized clusters might be useful to model completely covered surfaces, e.g., for studying direct ligand–ligand interactions. For comparison with surfaces at lower coverage on the other hand, studies of free TM clusters with a well defined but low number of ligands attached to their surface are needed.

This review is mainly concerned with systems where a single CO ligand is bound to an isolated TM cluster. The main emphasis is on the results of recent experiments in which the interaction of CO with TM clusters is investigated in the gas-phase by vibrational spectroscopy. This approach is made possible by the development of infrared multiple photon dissociation (IR-MPD) spectroscopy. In IR-MPD spectroscopy, fragmentation of the cluster–CO-complex, driven by a sequential resonant absorption of many IR photons, is monitored mass spectrometrically, and thus information on the IR absorption spectrum is obtained [14]. This method requires intense radiation sources emitting at the frequencies of the IR active vibrational modes. For a long time it was limited to a narrow wavelength range available from line-tunable CO₂ lasers around 10 μm [15]. The more recent development of

* Corresponding author. Tel.: +49 30 8413 5622; fax: +49 30 8413 5603.
E-mail address: fielicke@fhi-berlin.mpg.de (A. Fielicke).

infrared free electron lasers to produce tunable and intense radiation throughout the whole mid- and far-infrared has made IR-MPD a universal tool for structure determination of clusters in the gas-phase [16]. The approach has proven to be very successful for obtaining detailed structural information on, for instance, TM clusters [17–20], clusters of metal oxides [21–23], and metal cluster complexes [24–26]. IR-MPD spectroscopy can be applied to differently charged species (anions and cations), but also to neutrals and it is thus possible to study charging effects on the physical and chemical properties of the clusters.

This review is structured as follows. In Section 2 we briefly discuss kinetic and thermodynamic information on cluster–carbonyl complexes aiming to complement recent reviews on metal cluster–CO interactions [15,27,28], before concentrating, from Section 3 onwards, on results obtained from IR-MPD spectroscopy. In Section 3 we discuss periodic trends in molecular vs. dissociative adsorption. In Section 4 we deal with the sensitivity of the frequency of the CO stretch vibration, $\nu(\text{CO})$, to the binding geometries of carbon monoxide on the cluster surface. Finally, in Section 5, the dependence of $\nu(\text{CO})$ on the clusters' size and charge is analyzed in detail and used to estimate charge transfer due to support and co-adsorption effects.

2. Cluster reactivities and M_n –CO binding energies

The first survey of the reaction of CO with TM clusters dates back to 1987 when Cox, Kaldor, and coworkers published their comprehensive experimental study on neutral V, Fe, Co, Ni, Cu, Nb, Mo, Ru, Pd, W, Ir, and Pt as well as Al clusters containing up to 14 atoms [29]. Later work by Anderson, Rosén, and coworkers identified rather smooth changes of the reactivity of V, Nb, Ni, and Rh clusters with size [30–32] and found more pronounced variations for Cu and Au clusters [33,34]. Higher sticking probabilities point to an increased complex stability and might be related to electronic shell closures for particular complex sizes (see below). A comparative study on the CO adsorption by cationic and anionic Group 5 (V, Nb, Ta) as well as Group 9 (Co, Rh, Ir) TM clusters in an FT-ICR ion trap [35] showed clearly lowered reactivity for anionic Group 5 clusters containing less than ~20 atoms, whereas for larger clusters the differences between anions and cations disappeared. The reduced reactivity of the smaller Group 5 metal anions was explained by the repelling effect of the electron cloud extending from the cluster surface. This effect was not observed for the Group 9 metals since the extra electron can be more confined due to the higher electron affinity of the clusters.

For gas-phase clusters, quantitative data on CO binding energies are limited to only a few charged systems. The general trend is that the binding energies decrease with cluster size and that with growing size the CO binding strength converges to that of extended surfaces. This is especially the case for surface sites of low metal coordination. Quantitative information on CO binding energies is available for clusters of the coinage metals Cu [36], Au [37,38], and Au–Ag mixtures [39], as well as for Pt [40,41] and Pd [42] clusters. In general, binding energies for rather small clusters are already close to binding energies on extended metal surfaces. For instance, CO binds to anionic copper clusters in the size range of 3–7 atoms by about 0.6–0.9 eV [36]. This is comparable with the binding energies of CO on different sites of extended Cu surfaces, i.e., ~–0.5 eV on the terraces and –0.6 eV for step and kink sites [43]. The increase in bond strength from terrace to step or kink sites goes along with a decrease in the average coordination number N of the Cu atoms from 9 (for Cu(111)) to 6–7, respectively. For a small cluster, N is typically on the order of 3 or 4 which explains the observed stronger binding.

Enhanced stability of certain CO complexes is observed when the addition of the two electrons, formally donated from the CO ligand, leads to a particularly stable electronic structure, i.e., a complete filling of the clusters' valence shells. An enhanced binding energy has been found for Cu_5CO^- , which is taken to have in total 8 valence electrons. Similarly, increased stabilities have been reported for Cu_7CO^+ as well as for Cu_{16}CO and $\text{Cu}_{17}\text{CO}^+$ that have 8 and 18 valence electrons, respectively [33,44]. These stabilizations can be understood in the simple picture of electronic shell closures at 8 and 18 electrons within the “jellium” model of electrons bound by a spherical potential [45]. This clearly is a cluster specific stabilization mechanism.

3. Molecular vs. dissociative adsorption

The interaction of CO with a TM surface can lead to two fundamentally different products, a molecular adsorbate or the products of its dissociation, i.e., separated atomic O and C species. The fate of the CO molecule highly depends on the metal, its surface structure, and the reaction conditions. Vibrational spectroscopy provides a convenient method to distinguish between these two reaction channels not only for extended surfaces but also for isolated cluster complexes.

For a cluster complex of the stoichiometry $M_n\text{CO}$, the appearance of a vibrational band in the range of about 1400–2200 cm^{-1} unambiguously identifies the presence of molecular CO adsorbates since all other vibrational fundamentals for such systems, like internal cluster vibrations or M–O and M–C modes, are located significantly below 1400 cm^{-1} . The absence of such a band in the IR-MPD spectrum of a cluster complex on the other hand provides a strong indication for the dissociation of the CO molecule on the metal cluster since the carbonyl ligand has a large IR absorption cross section and the available IR laser power is sufficient to drive the IR-MPD process. We have investigated clusters of a large variety of TM with focus on their interactions with CO in the gas-phase. The results are summarized in Fig. 1 where the darker shaded fields indicate the investigated metals and the letters below the elemental sign denote the charge states of the clusters studied. For systems where different charge states have been investigated, no difference with respect to the molecular or dissociative CO binding is found.

For the early TM V, Nb, and Ta no $\nu(\text{CO})$ bands have been detected. However, a short-lived molecular CO adsorbate has been postulated to explain the reactivity of the neutral Nb_8 cluster towards H_2 and CO [46]. For Nb_3CO and $\text{Nb}_3(\text{CO})_2$, CO dissociation

21 Sc	22 Ti	23 V C	24 Cr	25 Mn	26 Fe N	27 Co ANC	28 Ni NC	29 Cu	30 Zn
39 Y	40 Zr	41 Nb N	42 Mo	43 Tc	44 Ru AC	45 Rh ANC	46 Pd AC	47 Ag NC	48 Cd
57 La	72 Hf	73 Ta N	74 W N	75 Re C	76 Os	77 Ir	78 Pt ANC	79 Au ANC	80 Hg

Fig. 1. Chemisorption behaviour of CO on TM clusters as identified by the presence or absence of $\nu(\text{CO})$ absorption bands in the cluster complex (complexes formed at ~300 K). Dark (orange) shading denotes verification of molecular chemisorption through the presence of $\nu(\text{CO})$ bands, while lighter shading (blue) designates the absence of any $\nu(\text{CO})$ bands indicating a dissociation of CO on the cluster surface. The remaining metals have yet to be studied. The bold line gives the borderline between molecular and dissociative adsorption on extended surfaces at ~300 K as suggested by Brodén[52]. The lettering specifies if the experiments have been performed on anionic (A), neutral (N), or cationic (C) clusters. More detailed discussions of the vibrational spectra for most of the metals have been reported elsewhere: V[80], Nb[47], Co[73], Rh[25,59,73], Ni[62,73], Pd[62], Pt[62], Au[70–72].

has been concluded both from ionization spectroscopy and from the absence of $\nu(\text{CO})$ bands in the IR-MPD spectra [47]. This finding is in agreement with the theoretical predictions for these systems. Large Nb_nCO species in the size range of $n = 4\text{--}40$ have been formed at room temperature or at -150°C and investigated via IR-MPD spectroscopy. Also here, the vibrational spectra do not give any evidence for the presence of undissociated CO on a Nb_n cluster, which points to a low barrier for C–O dissociation.

For the late TM clusters the observation of $\nu(\text{CO})$ bands clearly reveals that CO chemisorbs molecularly. In general, the frequency of these bands does not shift much with size for neutral clusters containing typically 5–30 atoms, whereas for cationic and anionic clusters a clear size convergence towards the frequencies for the neutral species is seen if the cluster size increases. The average frequencies of the $\nu(\text{CO})$ bands in neutral M_nCO complexes that have been assigned to CO atop bound to a single TM atom in the cluster are given in Table 1. The values of $\nu(\text{CO})$ increase towards the end of a row and towards the bottom of a column. This is in accordance with the evolution of $\nu(\text{CO})$ on extended surfaces although the cluster values are systematically lower by about 20–100 cm^{-1} . This reduction is probably related to the lower coordination of the metal atoms in the clusters which favours the π -backdonation. The periodic trend of $\nu(\text{CO})$ throughout the TM is even reproduced for the atomic carbonyls M-CO [48] which indicates that CO bonding to TM is dominated by local effects acting on an atomic scale.

The primary interaction between a TM surface and CO has been described as a mixing of the CO 5σ orbital with the surface d_{z^2} orbital and s orbitals, as well as a mixing of the CO 2π states with the metal $d_{xz,yz}$ states, with the latter interaction being dominant. Moving to the left in the periodic table of the elements results in a rise of the Fermi level and of the diffuseness of d-orbitals which leads to a higher electron density in the C–O-antibonding 2π orbital and eventually to dissociation [49]. Quantum mechanical calculations reproduce this trend [50,51], which qualitatively seems to hold also for gas-phase clusters. However, this picture seems to be oversimplified since the Fermi level determines the work function, which would translate into the ionization potential (IP) of an isolated cluster. It is well known that clusters show pronounced size-dependent variations in their IP which, within this model, contradicts the size-independence of $\nu(\text{CO})$ for CO adsorbed on neutral clusters.

Since CO exclusively dissociates on early TMs, while molecular CO ligands are stable on late TMs, naturally the question arises at what elements the transition occurs. For CO adsorbed on surfaces at room temperature this range has been identified already in the early work by Brodén [52] (the borderline shown in Fig. 1) and the general picture presented therein for the transition from dissociative to molecular CO binding still holds [53]: the transition shifts from the 3d metal Fe towards the early TM tungsten for the heavier 5d elements. Our preliminary results imply that at $\sim 300\text{ K}$ CO binds molecularly to Fe as well as to Co, Ru, and Re clusters [54]. For W they indicate a clear cluster size effect. Only for smaller W_n clusters with $n = 5\text{--}9, 11$ bands attributable to C–O stretch

vibrations are detectable, but these are missing for larger clusters implying that dissociation is taking place [54].

CO adsorption on iron surfaces forms a special case as at low coverage a highly red-shifted $\nu(\text{CO})$ at 1170 cm^{-1} is found on Fe(100) that has been attributed to a tilted or side-on bound CO [55]. This strongly activated CO adsorbate can be seen as a precursor state towards dissociation. For comparison, on neutral Fe clusters containing 13–30 atoms a broad $\nu(\text{CO})$ absorption feature around 1866 cm^{-1} is present for all cluster sizes [54]. A similar value is predicted for atop bound CO on Fe(100) by DFT calculations [56], but this is clearly lower than the $\sim 2100\text{ cm}^{-1}$ that are frequently assigned to atop CO on Fe(100). However, the cluster value for iron is fully in line with the general periodic trend of $\nu(\text{CO})$ as seen in Table 1. A possible explanation for the observation of a rather high $\nu(\text{CO})$ on the surface would be the formation of a geminal carbonyl on iron steps or adatoms on the surface.

4. Binding geometries

CO binding geometries on metal clusters can be determined from $\nu(\text{CO})$ by reference to long-standing experience on surfaces [8], taking into account that on clusters $\nu(\text{CO})$ is also a function of cluster size and charge. As the interaction of a CO molecule with multiple metal atoms leads to a more efficient $\text{M}\rightarrow\text{C}$ π backdonation and a significant weakening of the CO bond, $\nu(\text{CO})$ decreases typically by 100–150 cm^{-1} per additional M-C bond. These characteristic shifts in $\nu(\text{CO})$ allow for the identification of CO ligands in atop (μ_1), bridging (μ_2), or capping (μ_3) configurations.

In general, the majority of TM clusters is found to bind CO in an atop geometry. This is especially true in the low coverage limit, i.e., if just a single CO molecule binds to the cluster. This overall picture reproduces the adsorption behaviour of CO on surfaces at low coverage rather well. On closed packed TM surfaces CO binds usually in atop configurations, hollow sites are only favoured for Ni and Pd [51,57].

On 3d TM clusters CO binds nearly exclusively atop, including on most Ni clusters. Only for Ni_2CO and Ni_3CO , vibrationally resolved anion photoelectron spectra reveal rather low values of $\nu(\text{CO})$, $1800 \pm 80\text{ cm}^{-1}$ and $1750 \pm 80\text{ cm}^{-1}$, respectively, that suggest the presence of bridging CO ligands [58].

4d TM clusters present a larger variety of CO binding geometries with a tendency towards higher coordinating binding sites. Although atop binding is prevailing for CO on rhodium clusters, for some sizes and charge states, CO in bridging or hollow sites has been identified as well by IR-MPD spectroscopy (Fig. 2) [25,59]. For the higher coordination sites clear charge state dependence is observed, e.g., the CO binds in μ_3 configuration to the neutral and cationic Rh tetramer, while for the anion only μ_1 -binding is observed. For Rh_nCO clusters in the 10–15 atoms range, isomers with μ_1 - and μ_2 -binding are present. With increasing electron density, i.e., when going from the cationic over neutral to anionic clusters, the tendency to form a bridged carbonyl increases. There is no clear evidence for bridging CO in Rh_nCO^+ ($n = 10\text{--}15$), but the corresponding vibrational bands become visible for neutrals and even more pronounced for the anions where, for instance, for $n = 12$ and 13 the μ_1 - and μ_2 -bands have comparable intensities. In larger clusters, again, only atop binding is observed. A similar enhancement of bridged over atop binding with increasing charge is observed for supported Pt nanoparticles of 1–2 nm size [60]. In that study different supports have been used to vary the electron density on the metal. Covering a Rh surface with potassium effectively enhances electron density on the TM and is claimed to drive CO adsorption in higher coordination sites [61]. Furthermore, signatures of bridging and face-capping CO ligands are detected in the vibrational spectra of CO bound to clusters of the later 4d metal

Table 1

Average values for $\nu(\text{CO})$ (in cm^{-1}) assigned to atop (μ_1) CO ligands in neutral M_nCO complexes containing up to 30 metal atoms.

	Fe	Co	Ni	
	1865	1940	1994	
	Ru^a	Rh	Pd^a	Ag^b
	~ 1910	1960	~ 2000	2090
W			Pt	Au^c
1927			2020	2091

^a average of anionic and cationic clusters.

^b from Ag_5CO_3 .

^c from complexes that contain 3–5 CO ligands and 3–11 Au atoms.

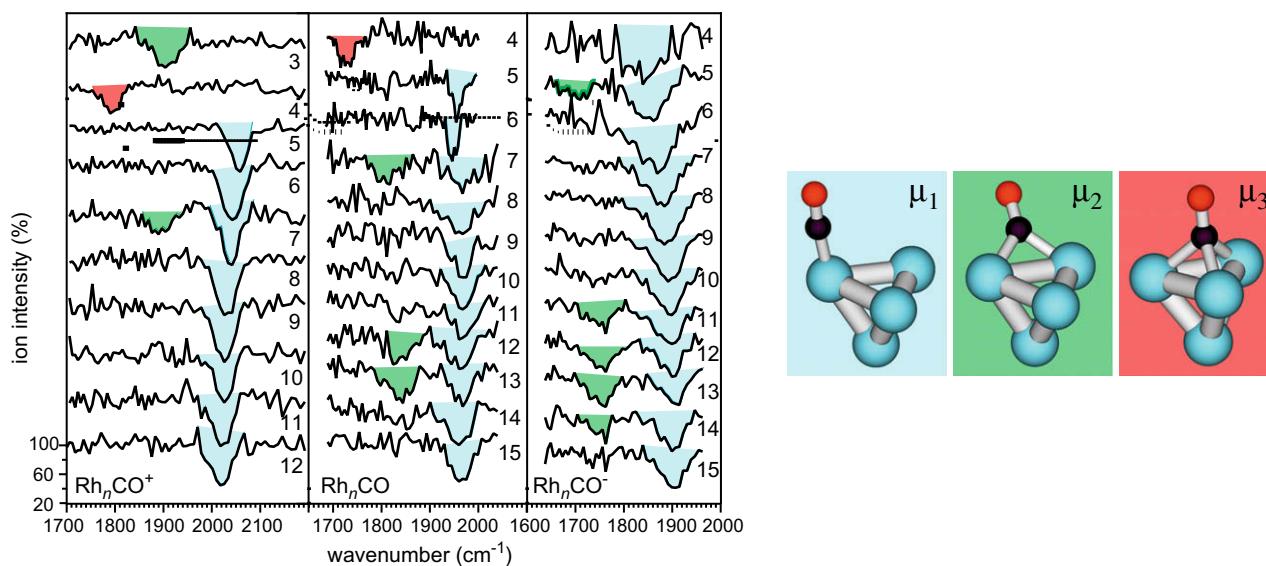


Fig. 2. IR spectra of $\text{Rh}_n\text{CO}^{+/0/-}$ in the range of the CO stretch vibration (left) and examples for different CO binding geometries on a cluster (right). For most clusters atop binding is observed, only for the smallest clusters exclusive μ_2 -bridging (Rh_3CO^+) or μ_3 -capping ($\text{Rh}_4\text{CO}^{+0}$) is found. For several clusters isomers with μ_1 -atop and μ_2 -bridging CO ligands are present.

palladium. Although for some clusters vibrational bands corresponding to atop CO are present, the higher coordinating CO ligands are the prevailing species for Pd [62]. Higher coordinated CO ligands are also observed on a few clusters of Ruthenium, the element preceding Rh and Pd in the row of 4d metals [54].

The trend towards higher coordinating binding sites prevails for the 5d TM clusters of tungsten and rhenium [54]. However, to clusters of the late 5d metal platinum CO binds only in atop configuration. In this case, relativistic effects must be taken into account in understanding the M–CO interaction. The preference of CO for atop binding on Pt surfaces has been explained before on the basis of relativistic gradient-corrected DFT calculations for CO bound to cluster models of the Ni, Pd, and Pt (100) surfaces [63]. If relativistic effects are not taken into account, the M–CO bond length would increase monotonically in the row $\text{Ni} < \text{Pd} < \text{Pt}$, related with a decrease in CO binding energy [64,65]. The M–CO distance shortens for Pd, and even more for Pt, if scalar relativistic corrections are applied. This goes along with a corresponding increase in the CO binding energies. Such contractions and the related stabilization due to relativistic effects are found, however, to be much smaller for bridging CO ligands. As a result, this leads to a stabilization of atop Pt–CO relative to bridge bound CO [63]. In the case of Pd, bridge bound CO ligands remain the more stable species. As the 5d orbitals are more spatially extended for the earlier 5d elements the destabilization of bridging CO ligands due to the relativistic effect is indeed expected to be lower in comparison to platinum.

The information on the vibrational properties of TM cluster–CO complexes allows reassessment of previous assumptions on CO binding geometries in such systems. For instance, based on the experimentally determined dissociation energies of Pt_nCO_m^- ($n = 3–6$, $m = 1–6$) it has been argued that the first CO binds in a bridging configuration [41]. More recent DFT studies [66], however, find atop binding in better agreement with the energetics. The spectroscopic results now confirm the assignment to atop bound carbonyl in Pt_nCO^- [62]. A second example is the prediction of the μ_2 -binding of CO to neutral Au_5 that is recurring in some theoretical studies [67–69]. Also in measurements of low-temperature matrix IR spectra of co-deposited Au and CO, a feature observed at 1853 cm^{-1} is suggested to be due to μ_2 -bound CO on Au_5 [68]. However, for cationic [70,71], anionic [72], or neutral gold cluster

carbonyls in the gas-phase, only atop bound CO is found without any signatures for higher coordinating CO.

Summing up, single CO molecules are found to bind to TM clusters in the atop configuration in most cases. Higher coordinating, i.e., bridging or face-capping CO ligands are only found for clusters of the 4d (Ru, Rh, Pd) and the earlier 5d (W, Re) metals. For the late 5d metal platinum, bridging CO ligands become less stable again due to relativistic effects.

5. Effects of electron density

Gas-phase clusters are convenient systems to study effects of electron density on the chemical properties as they can be prepared and investigated in different and precisely defined charge states, i.e., as neutral species and as singly charged cations or anions. For small clusters the effect of an excess electron or hole does not get strongly diluted by delocalization over the cluster, and the charge clearly influences the CO adsorption behaviour [59,72,73]. Effects of the cluster charge state on the CO binding geometry have been discussed before. Here, the focus will be on the effect of electron density on the strength of the carbonyl's internal C–O bond. The sensitivity of $\nu(\text{CO})$ to the metals' charge density makes it a common tool to probe the electronic properties of surface sites.

As the π -backdonation is an interaction of partially filled $M(\delta)$ orbitals with the empty $\text{CO}(2\pi)$ orbitals that are of C–O antibonding character, the C–O bond strength is related to the occupancy of the $M(\delta)$ orbitals. This leads to a dependence of the C–O bond strength and thereby also of $\nu(\text{CO})$ on the charge of the metal center. The values of $\nu(\text{CO})$ for single CO molecules bound to cationic, neutral, and anionic rhodium clusters and their dependence on cluster size are depicted in Fig. 3. While for neutral clusters $\nu(\text{CO})$ is nearly independent of cluster size, it decreases with growing size in the case of the cations and increases in the case of the anions, approaching the values for the neutral clusters. This behaviour can be understood by a simple charge dilution model [73] which is described briefly in the following.

For CO bound to a charged metal cluster it can be assumed that the occupancy $P(2\pi)$ of the $\text{CO}(2\pi)$ orbitals depends linearly on the fraction of the total cluster charge z -e that resides on the metal

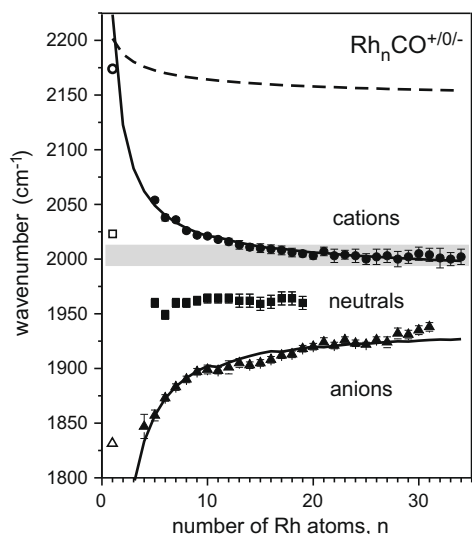


Fig. 3. Size and charge dependence of the $\nu(\text{CO})$ stretch frequency of μ_1 -bound CO in the mono carbonyl complexes of rhodium clusters. Open symbols are used for the atomic complexes in a Ne matrix (values from Ref. [89]). Details of the model that is used to describe the size dependence of $\nu(\text{CO})$ can be found in Ref. [73]. The range of $\nu(\text{CO})$ values for CO on Rh surfaces is indicated by the shaded area.

atom to which the CO binds. If the cluster charge is delocalized over all surface atoms, this fraction is inversely proportional to the number of surface atoms n_s in the cluster

$$P(2\pi) = P(2\pi)_\infty - \frac{\gamma Z}{n_s} \quad (1)$$

For large clusters, n_s is proportional to $n^{2/3}$; in small clusters one can estimate n_s by comparison with known cluster structures. A linear relationship between the calculated $\text{CO}(2\pi)$ orbital occupation $P(2\pi)$ and experimental $\nu(\text{CO})$ frequencies, in terms of the stretching force constants F_{CO} , has been established in earlier studies [74,75]

$$F_{\text{CO}} = F_{\text{free}} + \Delta F_{\text{ES}} - \beta P(2\pi) \quad (2)$$

F_{free} is the stretching force constant in the free CO molecule and β is the coefficient relating the $P(2\pi)$ occupation to the change of the force constant. An additional term ΔF_{ES} accounts for an electrostatic effect stemming from the interaction of the CO dipole with the electric field of the charged cluster [76,77]. The latter effect plays a significant but, compared to the influence of π -backdonation, minor role for the charge and size dependence of $\nu(\text{CO})$ in the TM cluster complexes. The stretching frequencies are then described by

$$\nu(\text{CO}) = \nu_\infty + \Delta\nu_{\text{ES}} + \frac{\gamma' Z}{n_s} \quad (3)$$

Details on the electrostatic effect in charged metal cluster carbonyls and a more rigorous derivation of Eq. (3) are given in Ref. [73]. This model describes the experimental data quite well (solid lines in Fig. 3). The contribution of the electrostatic effect $\Delta\nu_{\text{ES}}$ is shown separately by the dashed line. Following Eq. (3) one can expect $\nu(\text{CO})$ to shift linearly with the charge state for a cluster of a specific size. Indeed, such behaviour is found experimentally (Fig. 4).

The frequencies for the gas-phase cluster complexes can be compared to the ones for CO adsorbed on clusters of similar size interacting with a substrate in order to assess the electron density on the deposited metal particles. This leads to quantitative information on the charge transfer between metal cluster and substrate, e.g., from defect centers. In making such a comparison one must be

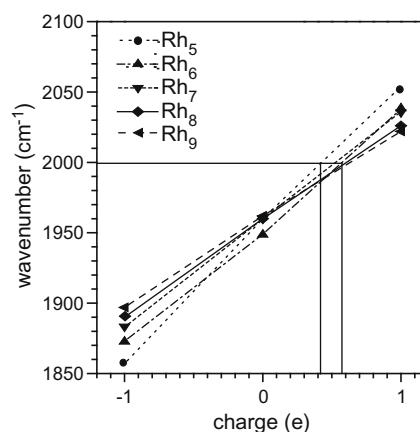


Fig. 4. Effect of charge on the $\nu(\text{CO})$ stretch frequency of μ_1 -bound CO in small rhodium cluster-CO complexes. The horizontal line indicates the observed $\nu(\text{CO})$ value of 2000 cm^{-1} for CO adsorbed on Rh clusters of similar size grown on highly ordered Al_2O_3 [13].

aware that the situation for a cluster interacting with a substrate surface is by far more complex than in the gas-phase. Interaction with the surface will lead to changes in the cluster geometries and the charge distribution within the cluster. Surface bound clusters may occupy different sites on the substrate, and often the CO coverage is not precisely known. As $\nu(\text{CO})$ depends on the surface coverage with CO, a comparison can only be made for similar coverage, i.e., at the low coverage limit. Additionally, the CO adsorption itself may induce changes in the charge distribution between metal and support [78]. Nevertheless, $\nu(\text{CO})$ for CO on deposited metal particles can be analyzed in terms of the (partial) charge of the CO binding site. Until recently, this has often been done by comparison with stable molecular carbonyl compounds, CO bound to ordered crystal surfaces, atomic M-CO complexes in rare-gas matrices, or with theory. Gas-phase clusters allow for including also the effect of particle size into such a comparison. For deposited Rh clusters containing on average 5–6 atoms on a highly ordered Al_2O_3 film [13] the comparison with the gas-phase data indicates a significant positive charging of clusters by about $+0.4 - +0.6 e$ (Fig. 4) [59]. A similar comparison has been used to assess the charging of small gold clusters deposited on defect-rich or defect-free MgO substrates [72] as well as for Ni and Pt clusters [62].

The electron density of a metal cluster cannot only be affected by interaction with a surface but also by species bound directly to the cluster. Co-adsorption of hydrogen and carbon monoxide onto 3d TM clusters has been investigated in more detail [79,80] inspired by the relevance of these systems in heterogeneous catalysis, e.g., for Fischer-Tropsch synthesis. Co-adsorbed H can affect the interaction of CO with the cluster via site blocking leading to a stabilization of molecular CO on an early transition metal like vanadium [80], but it is also found to alter the C-O bond strength. In most cases co-adsorption of hydrogen leads to an increase of the C-O bond strength and a blue-shift of $\nu(\text{CO})$, as illustrated in Fig. 5 for cationic cobalt clusters. Hydrogen is dissociating on the surface of the cobalt clusters [81] leading to a localization of 3d electron density into Co-H bonds. Co-adsorbed CO molecules are sensitive to that effect. Binding of atomic hydrogen reduces the d-electron density available for backdonation into the $\text{CO}(2\pi)$ orbitals leading to a reduced weakening of the internal C-O bond. Thus, the process of charge localization in Co-H bonds has a similar consequence for the $P(2\pi)$ occupation as a (partial) ionization of the cluster and can be quantized in a similar expression by an extension of Eq. (1).

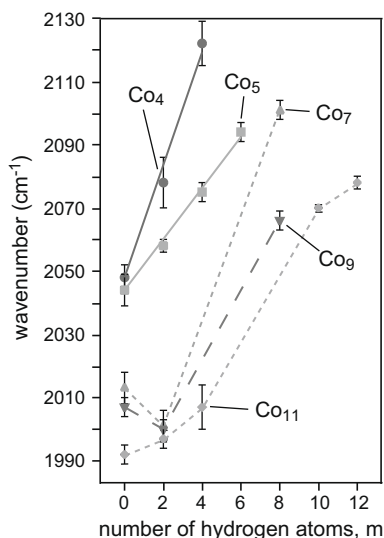


Fig. 5. Frequency of the C–O stretch vibration $\nu(\text{CO})$ of hydrogenated cobalt cluster carbonyls $\text{Co}_n(\text{CO})\text{H}_m^+$ as a function of the number of H atoms in the complex. The solid lines for $n = 4$ and 5 give fits of the data to Eq. (4).

$$P(2\pi) = P(2\pi)_\infty - \frac{\gamma Z}{n_S} - \frac{\gamma \sum_i^{n_H} \delta_i}{n_S} \quad (4)$$

Localization of electron density by binding the i th H atom is assumed to have the same effect as increasing the charge of a Co_nCO^+ complex by δ_i -e. If all co-adsorbed H atoms affect $\text{CO}(2\pi)$ in the same way it follows that

$$\nu(\text{CO}) = \nu(\text{CO})_0 - \frac{\gamma' n_H \delta}{n_S} \quad (5)$$

where $\nu(\text{CO})_0$ stands for $\nu(\text{CO})$ of the H-free carbonyl complex. The evaluation of plots as shown in Fig. 5 for cationic cobalt clusters containing 4–20 atoms yields average values for δ of about 0.09–0.25. The implication is that a single H atom bound to a cobalt cluster has the same effect on the electron density available for π -back-donation as 0.09–0.25 of a single positive charge. The close-to-linear dependence of $\nu(\text{CO})$ on the hydrogen atom coverage demonstrates that CO does not influence the charge transfer between the H-atoms and the cluster significantly. Therefore, CO can be used to probe changes of electron density induced by the co-adsorbed H atoms. Moreover, Eq. (5) underlines that $\nu(\text{CO})$ is sensitive to the relative coverage n_H/n_S and the model should hold for larger particles or even extended surfaces as well.

6. Conclusion and outlook

The results presented here testify to a renaissance of the cluster–surface analogy. This revival is driven by the development of new techniques to determine the structure of metal clusters and by the ever increasing capability of theory to handle larger and more complex systems. The goal of molecular-scale rational design of catalyst systems using input from cluster models requires detailed knowledge and understanding of structure–reactivity relationships.

Establishing the structure of gas-phase clusters has proved difficult in the past but several recent approaches are now showing significant success. These include the relatively new techniques of ion-mobility spectrometry [82,83] and gas-phase electron diffraction [84,85], and improvements in photoelectron detachment spectroscopy [86]. In addition, a far-infrared version of the IR-MPD technique described in this review is also now providing

structural information on clusters themselves through vibrational spectroscopy of their rare-gas complexes [17–20].

The success of all of these structure determination techniques relies heavily on theory, essentially density functional theory (DFT), to help the interpretation of experimental results. In addition, theory is being applied to more and more difficult cases and to model reactive systems. Calculations are now performed on supported clusters that include the support, the cluster itself, and reagent molecule(s) [87]. Gas-phase cluster complexes provide benchmark data for these efforts.

On the reactivity front, this review, which focuses on CO adsorption on transition metal clusters, shows how IR-MPD spectroscopy can be used to probe cluster–ligand interactions. A significant promise of IR-MPD is that it can unambiguously distinguish the identity of adsorbed species, and that it therefore affords direct insight into reactions taking place on cluster surfaces. The example of distinguishing dissociative vs. molecular CO adsorption demonstrates this for a single ligand, but it will also be possible to distinguish reactions taking place between co-adsorbed species. The technique is by no means limited to CO. Other ligands studied to date include NO[71], H_2O [26], NH_3 [24], H_2 and the H atom [81], from which it is evident that IR-MPD can also be applied to adsorbates with only modest oscillator strengths. In the near future systems of even weaker oscillator strengths can be investigated via intracavity techniques [88].

Acknowledgements

We gratefully acknowledge the support of the Stichting voor Fundamenteel Onderzoek der Materie (FOM) in providing beam time on FELIX. We would like to thank the FELIX staff for their skillful assistance, in particular Dr. A.F.G. van der Meer and Dr. B. Redlich. P.G. thanks the IMPRS “Complex Surfaces in Materials Science” for funding.

References

- [1] F.A. Cotton, Q. Rev. Chem. Soc. 20 (1966) 389.
- [2] E.L. Muetterties, T.N. Rhodin, E. Band, C.F. Brucker, W.R. Pretzer, Chem. Rev. 79 (1979) 91.
- [3] M.D. Morse, M.E. Geusic, J.R. Heath, R.E. Smalley, J. Chem. Phys. 83 (1985) 2293.
- [4] G. Frenking, N. Fröhlich, Chem. Rev. 100 (2000) 717.
- [5] M. Zhou, L. Andrews, C.W. Bauschlicher, Chem. Rev. 101 (2001) 1931.
- [6] G. Blyholder, J. Phys. Chem. 68 (1964) 2772.
- [7] M. Haruta, Catal. Today 36 (1997) 153.
- [8] N. Sheppard, T.T. Nguyen, in: R.E. Hester, R.J.H. Clark (Eds.), Advances in Infrared and Raman Spectroscopy, vol. 5, Heyden, London, 1978, p. 67.
- [9] F.M. Hoffmann, Surf. Sci. Rep. 3 (1983) 107.
- [10] U. Heiz, A. Sanchez, S. Abbet, W.-D. Schneider, Chem. Phys. 262 (2000) 189.
- [11] A.S. Wörz, K. Judai, S. Abbet, U. Heiz, J. Am. Chem. Soc. 125 (2003) 7964.
- [12] T. Dellwig, G. Rupprechter, H. Unterhalt, H.J. Freund, Phys. Rev. Lett. 85 (2000) 776.
- [13] M. Frank, M. Bäumer, R. Kühnemuth, H.-J. Freund, J. Phys. Chem. B 105 (2001) 8569.
- [14] J. Oomens, B.G. Sartakov, G. Meijer, G. von Helden, Int. J. Mass Spectrom. 254 (2006) 1.
- [15] M.B. Knickelbein, Ann. Rev. Phys. Chem. 50 (1999) 79.
- [16] K.R. Asmis, A. Fielicke, G. von Helden, G. Meijer, The chemical physics of solid surfaces, in: D.P. Woodruff (Ed.), Atomic Clusters: From Gas-Phase to Deposited, Elsevier, Amsterdam, 2007, p. 327.
- [17] A. Fielicke, A. Kirilyuk, C. Ratsch, J. Behler, M. Scheffler, G. von Helden, G. Meijer, Phys. Rev. Lett. 93 (2004) 023401.
- [18] C. Ratsch, A. Fielicke, A. Kirilyuk, J. Behler, G. von Helden, G. Meijer, M. Scheffler, J. Chem. Phys. 122 (2005) 124302.
- [19] A. Fielicke, C. Ratsch, G. von Helden, G. Meijer, J. Chem. Phys. 127 (2007) 234306.
- [20] P. Gruene, D.M. Rayner, B. Redlich, A.F.G. van der Meer, J.T. Lyon, G. Meijer, A. Fielicke, Science 321 (2008) 674.
- [21] K.R. Asmis, M. Brümmer, C. Kaposta, G. Santambrogio, G. von Helden, G. Meijer, K. Rademann, L. Wöste, PCCP 4 (2002) 1101.
- [22] M. Sierka, J. Döbler, J. Sauer, G. Santambrogio, M. Brümmer, L. Wöste, E. Janssens, G. Meijer, K.R. Asmis, Angew. Chem. Int. Ed. 46 (2007) 3372.
- [23] K.R. Asmis, J. Sauer, Mass Spectrom. Rev. 26 (2007) 542.
- [24] B. Simard, S. Dénommée, D.M. Rayner, D. van Heijnsbergen, G. Meijer, G. von Helden, Chem. Phys. Lett. 357 (2002) 195.

- [25] A. Fielicke, G. von Helden, G. Meijer, B. Simard, S. Dénoimée, D.M. Rayner, *J. Am. Chem. Soc.* 125 (2003) 11184.
- [26] T.D. Jaeger, A. Fielicke, G. von Helden, G. Meijer, M.A. Duncan, *Chem. Phys. Lett.* 392 (2004) 409.
- [27] K.M. Ervin, *Int. Rev. Phys. Chem.* 20 (2001) 127.
- [28] T.M. Bernhardt, *Int. J. Mass Spectrom.* 243 (2005) 1.
- [29] D.M. Cox, K.C. Reichmann, D.J. Trevor, A. Kaldor, *J. Chem. Phys.* 88 (1988) 111.
- [30] L. Holmgren, M. Andersson, A. Rosén, *Surf. Sci.* 331–333 (1995) 231.
- [31] M. Andersson, L. Holmgren, A. Rosén, *Surf. Rev. Lett.* 3 (1996) 683.
- [32] L. Holmgren, A. Rosén, *J. Chem. Phys.* 110 (1999) 2629.
- [33] L. Holmgren, H. Grönbeck, M. Andersson, A. Rosén, *Phys. Rev. B* 53 (1996) 16644.
- [34] N. Veldeman, P. Lievens, M. Andersson, *J. Phys. Chem. A* 109 (2005) 11793.
- [35] I. Balteanu, U. Achatz, O.P. Balaj, B.S. Fox, M.K. Beyer, V.E. Bondybey, *Int. J. Mass Spectrom.* 229 (2003) 61.
- [36] V.A. Spasov, T.-H. Lee, K.M. Ervin, *J. Chem. Phys.* 112 (2000) 1713.
- [37] G. Lüttgens, N. Pontius, P.S. Bechthold, M. Neeb, W. Eberhardt, *Phys. Rev. Lett.* 88 (2002) 076102.
- [38] M. Neumaier, F. Weigend, O. Hampe, M.M. Kappes, *J. Chem. Phys.* 122 (2005) 104702.
- [39] M. Neumaier, F. Weigend, O. Hampe, M.M. Kappes, *J. Chem. Phys.* 125 (2006) 104308.
- [40] A. Grushow, K.M. Ervin, *J. Am. Chem. Soc.* 117 (1995) 11612.
- [41] A. Grushow, K.M. Ervin, *J. Chem. Phys.* 106 (1997) 9580.
- [42] V.A. Spasov, K.M. Ervin, *J. Chem. Phys.* 109 (1998) 5344.
- [43] S. Vollmer, G. Witte, C. Wöll, *Catal. Lett.* 77 (2001) 97.
- [44] M.A. Nygren, P.E.M. Siegbahn, C. Jin, T. Guo, R.E. Smalley, *J. Chem. Phys.* 95 (1991) 6181.
- [45] W.A. de Heer, *Rev. Mod. Phys.* 65 (1993) 611.
- [46] Y. Xie, S.G. He, F. Dong, E.R. Bernstein, *J. Chem. Phys.* 128 (2008) 044306.
- [47] D.B. Pedersen, D.M. Rayner, B. Simard, M.A. Addicoat, M.A. Buntine, G.F. Metha, A. Fielicke, *J. Phys. Chem. A* 108 (2004) 964.
- [48] M. Zhou, L. Andrews, C.W. Bauschlicher Jr., *Chem. Rev.* 101 (2001) 1931.
- [49] S.S. Sung, R. Hoffmann, *J. Am. Chem. Soc.* 106 (1985) 578.
- [50] B. Hammer, J.K. Nørskov, *Adv. Catal.* 45 (2000) 71.
- [51] M. Gajdoš, A. Eichler, J. Hafner, *J. Phys.: Condens. Mater.* 16 (2004) 1141.
- [52] G. Brodén, T.N. Rhodin, C. Brucker, R. Benbow, Z. Hurych, *Surf. Sci.* 59 (1976) 593.
- [53] W. Andreoni, C.M. Varma, *Phys. Rev. B* 23 (1981) 437.
- [54] J.T. Lyon, P. Gruene, A. Fielicke, G. Meijer, D.M. Rayner, in preparation.
- [55] S.L. Bernasek, *Ann. Rev. Phys. Chem.* 44 (1993) 265.
- [56] D.C. Sorescu, D.L. Thompson, M.M. Hurley, C.F. Chabalowski, *Phys. Rev. B* 66 (2002) 035416.
- [57] F. Abild-Pedersen, M.P. Andersson, *Surf. Sci.* 601 (2007) 1747.
- [58] G. Ganteför, G. Schulze Icking-Konert, H. Handschuh, W. Eberhardt, *Int. J. Mass Spectrom. Ion Process.* 159 (1996) 81.
- [59] A. Fielicke, G. von Helden, G. Meijer, D.B. Pedersen, B. Simard, D.M. Rayner, *J. Phys. Chem. B* 108 (2004) 14591.
- [60] A.M.J. Van der Eerden, T. Visser, T.A. Nijhuis, Y. Ikeda, M. Lepage, D.C. Koningsberger, B.M. Weckhuysen, *J. Am. Chem. Soc.* 127 (2005) 3272.
- [61] J.E. Crowell, G.A. Somorjai, *Appl. Surf. Sci.* 19 (1984) 73.
- [62] P. Gruene, A. Fielicke, G. Meijer, D.M. Rayner, *Phys. Chem. Chem. Phys.* 10 (2008) 6144.
- [63] G. Pacchioni, S.-C. Chung, S. Krüger, N. Rösch, *Surf. Sci.* 392 (1997) 173.
- [64] S.-C. Chung, S. Krüger, G. Pacchioni, N. Rösch, *J. Chem. Phys.* 102 (1995) 3695.
- [65] J. Li, G. Schreckenbach, T. Ziegler, *J. Am. Chem. Soc.* 117 (1995) 486.
- [66] T. Santa-Nokki, H. Häkkinen, *Chem. Phys. Lett.* 406 (2005) 44.
- [67] N.S. Phala, G. Klatt, E. van Steen, *Chem. Phys. Lett.* 395 (2004) 33.
- [68] L. Jiang, Q. Xu, *J. Phys. Chem. A* 109 (2005) 1026.
- [69] E.M. Fernández, P. Ordejón, L.C. Balbás, *Chem. Phys. Lett.* 408 (2005) 252.
- [70] A. Fielicke, G. von Helden, G. Meijer, D.B. Pedersen, B. Simard, D.M. Rayner, *J. Am. Chem. Soc.* 127 (2005) 8416.
- [71] A. Fielicke, G. von Helden, G. Meijer, B. Simard, D.M. Rayner, *PCCP* 7 (2005) 3906.
- [72] A. Fielicke, G. von Helden, G. Meijer, B. Simard, D.M. Rayner, *J. Phys. Chem. B* 109 (2005) 23935.
- [73] A. Fielicke, G. von Helden, G. Meijer, D.B. Pedersen, B. Simard, D.M. Rayner, *J. Chem. Phys.* 124 (2006) 194305.
- [74] M.B. Hall, R.F. Fenske, *Inorg. Chem.* 11 (1972) 1619.
- [75] E.J. Baerends, P. Ros, *Mol. Phys.* 30 (1975) 1735.
- [76] A.S. Goldman, K. Krogh-Jespersen, *J. Am. Chem. Soc.* 118 (1996) 12159.
- [77] A.J. Lupinetti, S. Fau, G. Frenking, S.H. Strauss, *J. Phys. Chem. A* 101 (1997) 9551.
- [78] M. Sterrer, M. Yulikov, T. Risse, H.-J. Freund, J. Carrasco, F. Illas, C.D. Valentin, L. Giordano, G. Pacchioni, *Angew. Chem. Int. Ed.* 45 (2006) 2633.
- [79] I. Swart, A. Fielicke, D.M. Rayner, G. Meijer, B.M. Weckhuysen, F.M.F. de Groot, *Angew. Chem. Int. Ed.* 46 (2007) 5317.
- [80] I. Swart, A. Fielicke, B. Redlich, G. Meijer, B.M. Weckhuysen, F.M.F. de Groot, *J. Am. Chem. Soc.* 129 (2007) 2516.
- [81] I. Swart, F.M.F. de Groot, B.M. Weckhuysen, P. Gruene, G. Meijer, A. Fielicke, *J. Phys. Chem. A* 112 (2008) 1139.
- [82] A.A. Shvartsburg, R.R. Hudgins, P. Dugourd, M.F. Jarrold, *Chem. Soc. Rev.* 30 (2001) 26.
- [83] P. Weis, *Int. J. Mass Spectrom.* 245 (2005) 1.
- [84] D. Schooss, M.N. Blom, J.H. Parks, B.V. Issendorff, H. Haberland, M.M. Kappes, *Nano Lett.* 5 (2005) 1972.
- [85] X. Xing, B. Yoon, U. Landman, J.H. Parks, *Phys. Rev. B* 74 (2006) 165423.
- [86] J. Li, X. Li, H.-J. Zhai, L.-S. Wang, *Science* 299 (2003) 864.
- [87] B. Yoon, H. Häkkinen, U. Landman, A.S. Wörz, J.-M. Antonietti, S. Abbet, K. Judai, U. Heiz, *Science* 307 (2005) 403.
- [88] B.L. Militsyn, G. von Helden, G.J.M. Meijer, A.F.G. van der Meer, *Nucl. Instrum. Methods A* 507 (2003) 494.
- [89] M. Zhou, L. Andrews, *J. Am. Chem. Soc.* 121 (1999) 9171.